REMOTE SENS. ENVIRON. 41:105–121 (1992)

A Three-Dimensional Radiative Transfer Method for Optical Remote Sensing of Vegetated Land Surfaces

*R. B. Myneni**

Hydrological Sciences Branch, NASA/Goddard Space Flight Center, Greenbelt

G. Asrar

NASA Headquarters, Washington, DC

F. G. Hall

Biospheric Sciences Branch, NASA/Goddard Space Flight Center, Greenbelt

In the application of remote sensing at optical wavelengths to vegetated land surfaces from satellite-borne high-resolution instruments, such as those scheduled for the Earth Observing System, an understanding of the various physical mechanisms that contribute to the measured signal is important. In this context, numerical radiative transfer in three-dimensional coupled medium of atmosphere and vegetation has several applications, as in the development of correction routines for atmospheric perturbations, target information retrieval techniques, study of terrain elevation and adjacency effects, etc. A numerical method for solving the radiative transfer equation in three spatial dimensions was recently developed and analyzed for its numerical behavior. In this article, continued development of the method is reported, including an efficient acceleration algorithm. The reliability of coding and accuracy of the algorithm are evaluated by benchmarking. Parameterization of the method and results of a simulation are presented to document the utility of the code for applications in optical remote sensing studies of vegetated land surfaces. A simple model of the hot spot effect and sample calculations are presented. Finally, the radiative transfer method is tested with experimental data of vegetation canopy reflectance factors at two wavelengths.

INTRODUCTION

The problem of interpreting remotely sensed reflectance data and of associating a particular characteristic of the signal with some condition of the target requires an understanding of how the various physical mechanisms interact to produce the measured signal. In general, a multiplicity of processes participate and the problem of disentangling the various contributory effects is a central issue in remote sensing. For instance, in the application of remote sensing from satellite-based sensors to vegetated land surfaces, an understanding of the spectral response resulting from leaf internal microscopic structure and the perturba-

* Universities Space Research Association Resident Associate.

Address corespondence to R. B. Myneni, Hydrological Sciences Branch, NASA / GSFC, Mail Code 974, Greenbelt, MD 20771.

Received 1 March 1992.

0034-4257 / 92 / $5.00

655 Avenue of the Americas, New York, NY 10010

tions introduced by the macroscopic aggregation of leaves into a canopy and the intervening atmosphere is required. The physics of this problem is most convienently posed as a photon transport equation, the solution of which is the remote spectral measurement. Thus, numerical radiative transfer calculations can be useful in determining the key parameters of the target that contribute to the remote signal, their sensitivity to perturbations, and the situations under which the effect of a particular parameter is either maximum or minimum.

Past remote sensing studies of specific canopy attributes have used idealized canopy architectural features and transport formulations. In particular, the two- and four-flux methods have been quite popular because of the simplicity of the equation set (Suits, 1972; Bunnik, 1978; Dickinson, 1983; Verhoef, 1984; Sellers, 1985). In these moments formulations, the complete photon directional information is collapsed into a limited number of directions, usually two or four. The particle propagation equations and their coefficients are presented in a heuristic manner; however, Bunnik (1978) has given plausibility arguments for the nature of all the coefficients in the Suits (1972) model. Nevertheless, it can be verified by a proper integration of the transport equation that the linear differential equations are approximate (Myneni et al., 1989). This loss of rigor results in incorrect estimates of the moments; for example, the popular Suits model does not obey photon conservation and gives unrealistic results if the flux is incident purely as diffuse skylight (Gutschick and Wiegel, 1984). In spite of these caveats, these methods have provided a first understanding of the physical problem and are still widely used (Choudhury, 1987; Hall et al., 1990). A valuable review of these methods and other canopy reflection models can be found in Goel (1988).

On the other hand, attempts to solve the transport equation by rigorous numerical methods developed in astrophysics and reactor physics have been the subject of several works. Gutschick and Wiegel (1984) derived an exact integral equation for the azimuthally integrated radiation intensity and solved it numerically by iteration for randomly oriented, optically isotropic, plant canopies. It can be verified that the exact integral equation is essentially identical to that encountered in classical radiative transfer. Also for such ideal canopies, Gerstl and Zardecki (1985) solved the appropriate transfer equation using the discrete ordinates approximation in conjunction with a finite element method for the spatial derivatives. Later, Simmer and Gerstl (1985) used the Henyey–Greenstein model for scattering by leaves. These earlier important studies employed simple scattering kernels that resulted in rotationally invariant transport formulations. Shultis and Myneni (1988) examined a realistic leaf scattering phase function and derived explicit analytical results for the scattering kernels. In particular, they showed that rotationally invariant scattering kernels are not characteristic of vegetation canopies. Based on this realization, various modified forms of the governing transport equation for leaf canopies were derived. They also presented a modified discrete ordinates method that incorporates the direction-dependent cross sections. Marshak (1989) continued this theoretical development by including specular reflection and the hot spot effect through modified cross sections. These methods have been quite successful in terms of satisfactory agreement with experimental data and for providing a rigorous basis for the physics of photon interaction with leaf canopies. A review of the various methods of solving the refractory transport equation can be found in Myneni et al. (1989).

A majority of the numerical methods of solution of the transport equation are in the context of a horizontally homogeneous and laterally infinite plant stands. However, most natural vegetation communities are horizontally heterogeneous and require a three-dimensional treatment. The Monte Carlo method developed by Ross and Marshak (1988) is applicable to laterally heterogeneous plant stands. This method permits a realistic description of canopy architecture but is computer-intensive and difficult to parameterize. The geometrical–optical approach of Li and Strahler (1986) idealizes the 3D scene as fractional areas of empirical quantities termed component brightnesses. Also, the method is poorly applicable in the strongly scattering region of the spectrum. The 3D model developed by Welles and Norman (1991) represents individual foliage envelopes as geometrical solids of constant leaf area density, and multiple scattering is treated as a two-flux problem. The method developed by

Kimes and Kirchner (1982) is similar to the discrete ordinates method in that photons are restricted to travel in a finite number of directions. However, these directions are selected by dividing the polar coordinates into a fixed number of equispaced intervals. The resulting quadrature set is clearly inferior to the S_N or the EQ_N set in terms of evaluating the angular integrals. Also, the scattered intensity originating in a spatial cell is assumed to stream without interaction to the neighboring cells, which can lead to errors for large spatial cells.

The above three-dimensional methods are approximate in their treatment of the physical problem. The conceptualization of the plant stand and the photon–vegetation interaction is not rigorously represented as in transport theory. For instance, these methods cannot be extended to study the coupled medium of atmosphere / vegetation transport problem. Also, corrections for atmospheric perturbations, adjacency and terrain elevation effects, target information retrieval techniques from data gathered at orbital altitudes, all require a 3D description of photon travel in the coupled atmosphere / vegetation medium. Hence, we developed a 3D radiative transfer method applicable for optical remote sensing of vegetated land surfaces as a first step. We are now using these codes to evaluate bidirectional reflectance factors to be used as boundary conditions in atmospheric radiative transfer problems.

In an earlier article (Myneni et al., 1990), the governing equation of transfer, cross sections, and a modified discrete ordinates method for numerical solution of the transfer equation for a three-dimensional leaf canopy were formulated. Models for the total interaction and scattering cross sections were presented, and preliminary transport calculations were also reported. Convergence acceleration of the iteration on the scattering source using the coarse mesh rebalancing method and convergence criteria were discussed. The extent of flux distortions such as negative and oscillatory fluxes, ray effects, etc., was assessed, and correction routines for these maladies were developed.

In this paper, the 3D method is briefly described, and a new acceleration technique for convergence of the iterative solution presented. The reliability of coding and accuracy of the discrete ordinates algorithm is assessed by reporting on some benchmark problems. Parameterization of the method and results of a simulation are presented to document the utility of the method for remote sensing applications. A simple model of the hot spot effect and sample calculations are presented. Finally, the radiative transfer method is tested with experimental data of vegetation canopy reflectance factors at two different wavelengths.

DISCRETE ORDINATES METHOD IN 3D CARTESIAN GEOMETRY

Statement of the Problem: The steady-state monochromatic intensity distribution function $I(\vec{r},\Omega)$ in the absence of polarization, frequency shifting interactions, and radiation sources within the canopy, is given by the radiative transfer equation (Myneni et al., 1990)

$$\Omega\bullet\vec{\nabla}I(\vec{r},\Omega)+\sigma(\vec{r},\Omega)I(\vec{r},\Omega)=\int_{4\pi}d\Omega'\ \sigma_s(\vec{r},\Omega'\rightarrow\Omega)I(\vec{r},\Omega'). \quad (1)$$

The position vector $\vec{r}$ denotes the triplet (x,y,z) with $0\leqslant x\leqslant X_s$, $0\leqslant y\leqslant Y_s$, and $0\leqslant z\leqslant Z_s$, and where X_s, Y_s, and Z_s are the dimensions of the canopy. The unit direction vector Ω has an azimuthal angle ϕ measured counterclockwise in the (x,y) plane from the positive X-axis, and a polar angle $\theta=\cos^{-1}(\mu)$ with respect to the outward normal. The streaming operator of radiation intensity $[\Omega\bullet\vec{\nabla}]$ is the spatial derivative along the path of photon flight (Lewis and Miller, 1984).

The total interaction cross section σ is defined such that the probability that a photon while traveling a distance ds hits a leaf is $\sigma(\vec{r},\Omega)\ ds$ (Shultis and Myneni, 1988) and depends on the leaf area density distribution $u_L(\vec{r})$ and the leaf normal orientation distribution $[2\pi^{-1}g_L(\vec{r},\Omega_L)]$. The differential scattering cross section $\sigma_s(\vec{r},\Omega'\rightarrow\Omega)$ may be expressed in terms of a leaf scattering phase function $\gamma_L(\Omega_L,\Omega'\rightarrow\Omega)$. For a leaf with outward normal Ω_L, this phase function is the fraction of the intercepted energy, from photons initially traveling in direction Ω', that is scattered into a unit solid angle about direction Ω. The volumetric rate at which photons traveling in Ω' are scattered into a unit solid angle about Ω, by leaves at $\vec{r}$ of all orientations Ω_L, equals the differential scattering cross section (Myneni et al., 1990). It can be seen that in addition to u_L and g_L, the leaf scattering

phase function γ_L must also be specified in order to furnish a complete description of radiation transport in leaf canopies.

The Method of Solution: The standard discrete ordinates method with some modifications can be employed to numerically solve the transfer equation (1) for the radiation intensity $I(\vec{r},\Omega)$. The discrete ordinates method in its current form was primarily developed in the context of neutron transport for reactor design and shielding purposes. This method is certainly the most popular method in numerical transport calculations as evidenced by its use (Carlson and Lathrop, 1968; Lathrop, 1976; Lewis and Miller, 1984). Its popularity can be explained by the fact that it is relatively easy to design algorithms that satisfy photon conservation, positivity, homogeneity, and stability of the solution. Details on the application of the discrete ordinates method for numerical solution of the plant canopy transport equation can be found in Myneni et al. (1990), where the emphasis was on the various maladies afflicting the numerical solution (viz., cell effects, oscillatory distortions of emergent radiations, ray effects, negative angular fluxes, etc.); methods to alleviate these deleterious effects were also developed.

DIFFUSION-SYNTHETIC ACCELERATION METHOD

The discrete ordinates equations are solved by the method of iteration on the scattering source. Convergence of this iteration is slow in optically deep canopies and in situations where the single scattering albedo is close to unity, viz., in the near-infrared wavelengths, because of multiple collisions. Hence, it is desirable to accelerate convergence of the iteration on the scattering source. The coarse mesh rebalancing technique is the most commonly used method to accelerate convergence (Lathrop, 1976). The principle of this method is simple. Since converged solutions must obey the particle conservation equation, convergence acceleration may be achieved by artificially enforcing particle balance over coarse regions in the particle domain. The effect of rebalancing is to bring flux amplitudes close to their final values, while subsequent iterations refine their shape.

We have employed the coarse mesh rebalancing method in the numerical solution of the 3D plant canopy radiative transfer equation. Our results indicate that this method results in significant convergence acceleration of the iteration on the scattering source (Myneni et al., 1990). However, in the case of horizontally infinite (but inhomogeneous) canopies, this method results in poor acceleration because of strong source strength. For such cases, we have resorted to an alternate acceleration method based on diffusion theory which we describe here.

In this method diffusion theory, that is, a lower order approximation, is used to accelerate convergence of the iteration on the source terms (Alcouffe, 1990). We begin by considering the transport equation

$$\Omega\bullet\vec{\nabla}I(\vec{r},\Omega)+\sigma(\vec{r},\Omega)I(\vec{r},\Omega)=\int_{4\pi}d\Omega'\ \sigma_s(\vec{r},\Omega'\rightarrow\Omega)I(\vec{r},\Omega')+Q'(\vec{r},\Omega),$$

where Q' is an external source. The iteration on the distribution source can be written in operator notation as

$$\Lambda^0\hat{I}^l=\Lambda^1 I^l+Q', \tag{2}$$

where l is the iteration index and $\hat{I}$ denotes the unaccelerated intensities. To derive the synthetic acceleration method, we integrate Eq. (2) over Ω:

$$\int_{4\pi}d\Omega\ [\Lambda I=Q']\equiv\int_{4\pi}d\Omega\ \Lambda I=Q;\quad\int_{4\pi}d\Omega\ Q'=Q, \tag{3}$$

where $\Lambda=\Lambda^0-\Lambda^1$. The operator Λ can be written in terms of a lower order diffusion operator Λ_D and a remainder $(\Lambda-\Lambda_D)$, and after some manipulation there results

$$\Lambda_D F_s=Q-\int_{4\pi}d\Omega\ (\Lambda-\Lambda_D)I, \tag{4}$$

where F_s is the scalar flux

$$F_s(\vec{r})=\int_{4\pi}d\Omega\ I(\vec{r},\Omega).$$

For acceleration purposes Eq. (4) may be written as

$$\Lambda_D F_s^{l+1}=Q-\int_{4\pi}d\Omega\ (\Lambda-\Lambda_D)\hat{I}^l. \tag{5}$$

Combining Eqs. (5) and (2) and noting that $\Lambda=\Lambda^0-\Lambda^1$, we obtain

$$F_s^{l+1}=\hat{F}_s^l+\Lambda_D^{-1}\int_{4\pi}d\Omega\ \Lambda^1(I^l-\hat{I}^l).$$

The quantities $\hat{F}_s^l$, $\hat{I}^l$, and I^l are known from discrete ordinates calculations. The inverse of the diffusion operator is known from a solution of the corresponding diffusion equation (Pomraning, 1973). Hence, $\hat{F}_s^{l+1}$, may be calculated. The iteration clearly converges as $\hat{I}^l \to I^l$. The diffusion-synthetic acceleration methods are more sensitive to spatial mesh spacing than the coarse mesh rebalancing methods. However, when the synthetic method is stable, it produces acceleration that is superior than the coarse mesh rebalancing method. The results presented in the next section were obtained with the use of this acceleration method.

BENCHMARKING OF THE 3D CODE

The results presented in this section are designed to demonstrate the reliability of coding and accuracy of the 3D discrete ordinates algorithm. For the case of horizontally homogeneous plant canopies of infinite lateral extent, results of the 3D code should agree with solutions of the one-dimensional transport equation because the horizontal divergence of the intensity distribution is zero.

We begin by assuming that the 3D plant canopy segment of dimensions, $0 \leqslant x \leqslant X_s$, $0 \leqslant y \leqslant Y_s$, and $0 \leqslant z \leqslant Z_s$, is representative of the horizontally infinite canopy. Thus, photons exiting the system from one edge can be assumed to be incident on the opposite edge, with the other phase-space coordinates held constant. In this manner a horizontally infinite canopy can be simulated, thus restricting photons to enter / exit the system at the top and bottom surfaces only. For such a configuration, the boundary conditions to Eq. (1) are specified in the following way.

As is customary in radiative transfer, we begin with the separation of uncollided radiation field I^o from the intensity I^c of photons scattered one or more times in the canopy. Let the intensity at a point in the phase space be $I(\vec{r},\Omega) = I^o(\vec{r},\Omega) + I^c(\vec{r},\Omega)$. The equation of transfer for the uncollided radiation field is

$$\Omega \bullet \vec{\nabla} I^o(\vec{r},\Omega) + \sigma(\vec{r},\Omega) I^o(\vec{r},\Omega) = 0. \tag{6}$$

Let the leaf canopy be illuminated from above by both a monodirectional solar component [in the direction $\Omega_o \sim (\mu_o,\phi_o)$, $\mu_o < 0$; of intensity I_o] as well as by diffuse radiation from the sky [in directions $\Omega \sim (\mu,\phi)$, $\mu < 0$; of intensity I_d]. Therefore, the incident radiation field at the top of the canopy $(x,y,0)$ is

$$I^o(x,y,0;\Omega) \equiv I_d(\Omega) + I_o \delta(\Omega - \Omega_o), \quad \mu < 0.$$

At the bottom of the canopy (x,y,Z_s), a fraction r_s is assumed to be reradiated back into the canopy by the ground according to the soil BRDF γ_s, that is,

$$\begin{aligned} I^o(x,y,Z_s,\Omega) = {} & \frac{\gamma_s(\Omega_o,\Omega)}{\pi} |\mu_o| I_o \\ & \times \exp\left\{ \frac{1}{\mu_o} \int_0^{Z_s} dz' \ \sigma[\vec{r}'(\Omega_o),\Omega_o] \right\} \\ & + \frac{1}{\pi} \int_0^{2\pi} d\phi' \int_{-1}^{0} d\mu' \ \gamma_s(\Omega',\Omega) |\mu'| I_d(\Omega') \\ & \times \exp\left\{ \frac{1}{\mu'} \int_0^{Z_s} dz' \ \sigma[\vec{r}(\Omega'),\Omega'] \right\}, \quad \mu > 0. \end{aligned}$$

The solution of the radiative transfer equation (6) subject to these boundary conditions is as follows: For $\mu < 0$,

$$\begin{aligned} I^o(\vec{r},\Omega) = {} & I_o \ \exp\left[\frac{1}{\mu} \tau_1(\vec{r},\Omega) \right] \delta(\Omega - \Omega_o) \\ & + I_d(\Omega) \ \exp\left[\frac{1}{\mu} \tau_1(\vec{r},\Omega) \right], \end{aligned}$$

and for $\mu > 0$,

$$I^o(\vec{r},\Omega) = I^o(x,y,Z_s,\Omega) \ \exp\left[-\frac{1}{\mu} \tau_2(\vec{r},\Omega) \right].$$

In the above, the optical depths τ_1 and τ_2 are

$$\tau_1(\vec{r},\Omega) = \int_0^z dz' \ \sigma[\vec{r}'(\Omega),\Omega],$$

$$\tau_2(\vec{r},\Omega) = \int_z^{z_s} dz' \ \sigma[\vec{r}'(\Omega),\Omega].$$

The equation of transfer for the collided radiation field is

$$\begin{aligned} & \Omega \bullet \vec{\nabla} I^c(\vec{r},\Omega) + \sigma(\vec{r},\Omega) I^c(\vec{r},\Omega) \\ & = \int_{4\pi} d\Omega' \ \sigma_s(\vec{r},\Omega' \to \Omega) I^c(\vec{r},\Omega') + Q(\vec{r},\Omega), \end{aligned} \tag{7}$$

where the first collision source Q is

$$Q(\vec{r},\Omega) = \int_{4\pi} d\Omega' \ \sigma_s(\vec{r},\Omega' \to \Omega) I^o(\vec{r},\Omega').$$

The boundary conditions for Eq. (7) are vacuum

conditions on all sides of the leaf canopy except at the ground interface,

$$I^c(x,y,Z_s;\Omega) = \frac{1}{\pi}\int_0^{2\pi} d\phi' \times \int_{-1}^{0} d\mu'\ \gamma_s(\Omega',\Omega)|\mu'|I^c(x,y,Z_s;\Omega'), \quad \mu > 0.$$

We had earlier developed a discrete ordinates code for numerical solution of the 1D leaf canopy transport equation (Shultis and Myneni, 1988). Recently this code was tested against a highly accurate semianalytical method of solution of the transport equation (Ganapol and Myneni, 1991). For the problems investigated, the results of the 1D discrete ordinates code were found to be four digit accurate. In the following analysis we shall use the 1D code as a benchmark.

Consider a leaf canopy of dimensions 10 m × 10 m × 10 m. Let $u_L(\vec{r}) \equiv u_L = L/Z_s$, where L is leaf area index and Z_s is depth of the canopy. Assume that the probability density function of leaf normal orientation is invariant in canopy space, that is, $g_L(\vec{r},\Omega_L) \equiv g_L(\Omega_L)$. Thus $\sigma(\vec{r},\Omega) \equiv \sigma(\Omega)$. Specular reflection at the leaf surface is modeled by Fresnel equations averaged over polarization states, but corrected for leaf optical roughness (Myneni et al., 1990). Refractive index of the leaf cuticular wax layer is assumed wavelength-independent and equal to 1.5 (Vanderbilt and Grant, 1985). Scattering from leaf interior is modeled as a bi-Lambertian function following Shultis and Myneni (1988). With these models, the differential scattering cross section is also invariant of the positional variables, that is, $\sigma_s(\vec{r}; \Omega' \rightarrow \Omega) \equiv \sigma_s(\Omega' \rightarrow \Omega)$.

A horizontally infinite canopy was simulated with the finite canopy block by insuring that photons exiting the canopy from the sides were incident on the opposite side. The cross sections σ and σ_s were evaluated numerically with a 12-point Gauss quadrature. The results reported here were obtained with an EQ_6 quadrature set, that is, a total of 48 directions in the unit sphere.

Table 1 shows a comparision of canopy reflectance in the red (0.6–0.7 μm) and near-infrared (0.8–1.1 μm) region of the spectrum for different leaf angle distributions. The azimuthal distribution of leaf normals was assumed uniform; the inclination distribution was modeled as planophile, erectophile, plagiophile, extremophile, and uniform-based on data from de Wit (1965). The incident flux density was assumed 1 W m^{-2}, with 100% monodirectional beam irradiation along $\mu_o = -1.0$ and $\phi_o = 0.0$. Additionally, vacuum boundary conditions were assumed. The results indicate that the 3D method overestimates canopy reflectance; more so in the red region (2.1–3.6%) than in the near-infrared (0.5–0.9%).

Table 2 shows a comparision of canopy reflectance in the red and near-infrared for canopies with constant leaf angle illuminated by flux incident purely as diffuse isotropic skylight. The 3D results are greater than the 1D results and the difference is greater in the red region (4.8–13.7%) than in the near-infrared region (4.7–8.9%). Interestingly, the degree of overestimation increases with the mean leaf angle for both direct and diffuse illumination cases.

Table 3 shows a comparision of simulated reflected intensities in the near-infrared from canopies with erectophile inclination distribution, of

Table 1. Comparison of Canopy Albedos between the 3D and 1D Discrete Ordinates Codes[a]

Leaf Inclination Distribution	*Leaf Optical Properties*		*Canopy Albedo*	
	Reflectance	*Transmittance*	*3D Code*	*1D Code*
Erectophile	0.07	0.03	0.01391	0.01343
	0.45	0.45	0.14908	0.14783
Planophile	0.07	0.03	0.02712	0.02644
	0.45	0.45	0.25602	0.25415
Plagiophile	0.07	0.03	0.02169	0.02097
	0.45	0.45	0.21662	0.21540
Extremophile	0.07	0.03	0.02067	0.02025
	0.45	0.45	0.19747	0.19578
Uniform	0.07	0.03	0.01656	0.01605
	0.45	0.45	0.17045	0.16957

[a] The problem parameters are: LAI = 1.0; $\theta_o = 180°$; $\phi_o = 0°$ (also see the text).

Table 2. Comparison of Canopy Albedos between the 3D and 1D Discrete Ordinates Codes[a]

Mean Leaf Angle (deg)	Leaf Optical Properties		Canopy Albedo	
	Reflectance	Transmittance	3D Code	1D Code
7.21	0.07	0.03	0.03219	0.03072
	0.45	0.45	0.29683	0.28364
25.85	0.07	0.03	0.03007	0.02823
	0.45	0.45	0.28615	0.27416
45.59	0.07	0.03	0.02530	0.02335
	0.45	0.45	0.26836	0.25576
64.15	0.07	0.03	0.02056	0.01826
	0.45	0.45	0.25655	0.23557
82.79	0.07	0.03	0.01694	0.01491
	0.45	0.45	0.23952	0.22058

[a] The problem parameters are: LAI = 1.0; 100% isotropic skylight incidence (also see the text).

leaf area index 3, and illuminated by a monodirectional beam source. The 3D results are underestimates with a maximum discrepency of 3.1% for a view zenith angle of 75.16°. In general, the discrepency between the two methods is least for near-nadir view angles.

When scattering from canopies is isotropic, the emergent radiations should be azimuth-independent. This is illustrated in Table 4 where exiting near-infrared intensities from a canopy of leaf area index 3 under perpendicular monodirectional incidence are given. Again, the 3D results are lower than the 1D results, with a maximum difference of 3.1% at a view angle of 75.16°, and with smaller discrepencies at lower view zenith angles.

In view of the above results, we conclude that errors in our 3D code are directly correlated with mean leaf angle, portion of diffuse skylight in the incident flux, and inversely related to leaf area index and the single scattering albedo. Further, the emerging intensities in oblique directions are more suspect than those in near-nadir directions.

Table 3. Comparison of Emerging Intensities between the 3D and 1D Discrete Ordinates Codes[a]

View Direction		Exiting Radiance ($W\ m^{-2}\ sr^{-1}$)	
θ (deg)	ϕ (deg)	3D Code	1D Code
21.24	45.0	0.08302	0.08404
47.03	68.66	0.09174	0.09323
75.16	74.63	0.10434	0.10706
47.03	21.34	0.09187	0.09305
74.55	45.0	0.10483	0.10680
75.16	15.37	0.10387	0.10659
21.24	135.0	0.08303	0.08451
47.03	158.66	0.09175	0.09386
75.16	164.63	0.10434	0.10704
47.03	111.34	0.09189	0.09361
74.55	135.0	0.10483	0.10715
75.16	105.35	0.10388	0.10718
21.24	225.0	0.08303	0.08451
47.03	248.66	0.09175	0.09361
75.16	254.63	0.10434	0.10718
47.03	201.34	0.09189	0.09386
74.55	225.0	0.10483	0.10715
75.16	295.35	0.10388	0.10706
21.24	315.0	0.08302	0.08404
47.03	338.66	0.09174	0.09305
75.16	344.63	0.10434	0.10659
47.03	291.34	0.09187	0.09329
74.55	315.0	0.10483	0.10680
75.16	385.37	0.10387	0.10706

[a] The problem parameters are: LAI = 3.0; $\theta_o = 180°$; $\phi_o = 0°$; erectophile leaf inclination; leaf reflectance = transmittance = 0.45 (also see the text).

PARAMETERIZATION AND EXAMPLE RESULTS

In the second section it was shown that, in order to obtain a numerical solution of the 3D transport

Table 4. Comparison of Emerging Intensities between the 3D and 1D Discrete Ordinates Codes[a]

View Zenith Angle (deg)	Exiting Radiances ($W\ m^{-2}\ sr^{-1}$)	
	3D Code	1D Code
27.24	0.08788	0.09019
47.03	0.10023	0.10295
74.55	0.12099	0.12489
75.16	0.12134	0.12526

[a] The problem parameters are: optical depth = 1.5; single scattering albedo = 0.9; $\theta_o = 180°$; $\phi_o = 0°$; isotropic phase function; vacuum boundary conditions.

equation (1), we require information on the leaf area density function u_L, the probability density function of leaf normal orientation g_L, and the leaf scattering phase function γ_L. Once these functions are parameterized either by models or with empirical data, the cross sections σ and σ_s can be evaluated accurately by numerical quadrature. In this section we discuss parameterization of these functions and present results of a simulation to highlight the utility of the 3D code.

Leaf Area Density

We assume that the dimensions of the simulated plant canopy are representative of the actual plant stand. Thus, the entire plant stand can be simulated by lateral replication of the truncated canopy block. Let N_p denote tree density, with trees distributed in a certain fashion on the ground. This distribution could be random, regular, clumped, etc. We now wish to analytically describe the function u_L in the canopy space. One simple approach is to assume that u_L is uniformly distributed (Kimes and Kirschner, 1982). Another approach is to approximate the shape of a tree by an ellipsoid (Welles and Norman, 1991) or a cone (Li and Strahler, 1986), and assume that u_L is constant inside this shape. Most experimental data, however, indicate that this assumption is not valid (Ross, 1981). We had earlier developed a model for u_L for a leaf canopy consisting of N_p trees, where u_L of each tree was assumed given by a quadratic expression in $\vec{r}$ (Myneni et al., 1990). This quadratic model is simple but is nevertheless not characteristic of many tree stands. Therefore, we developed a computer-graphics-based model of a tree using fractal geometry from which u_L can be numerically evaluated (Myneni et al., 1990). Radiation regime simulated using fractal geometry for leaf area density distribution in a poplar stand agreed well with measurements (Myneni, 1991).

We consider a hypothetical stand of dimensions 16 m × 16 m × 10 m, with nine trees; spacing between trees is 6 m along both horizontal coordinates. The mean dimensions of the tree are 4 m × 4 m × 10 m. The simulated stand is shown in Figure 1. For simulation of fractal trees the following inputs were specified: total number of branchings—12; number of branchings before leaves grow—2; initial and final rotation angles in degrees—roll (130 and 100), pitch (50 and 30), and yaw (10 and 10); height of trunk—4 m; leaf shape—elliptical; leaf maximum length and width—0.12 m and 0.06 m; length of the petiole—0.04 m; phyllotaxy in degrees—144; distance between leaves on the branch—0.08 m. These values were treated as mean, and a random deviation of 10% was allowed in the simulation. The leaf area index of the trees varied from 9.66 to 11.86; leaf area index of the canopy is 6.86.

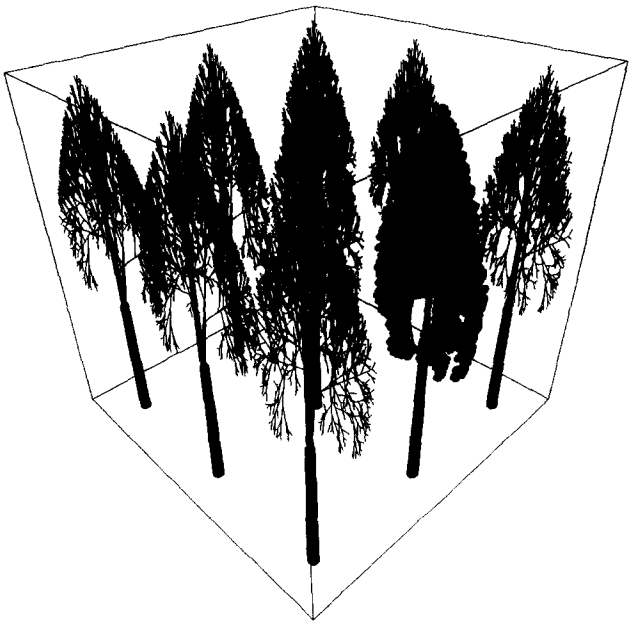

Figure 1. A tree stand simulated using fractal theory. The dimensions of the stand are $X_s - Y_s = 16$ m, and $Z_s = 10$ m. Within this enclosure, nine trees are regularly distributed at a spacing of 6 m. Only a single tree is drawn with leaves for reasons of computational economy. The parameters used in the simulation of trees are discussed in the text.

A fine spatial grid ($50 \times 50 \times 50$) is imposed on the stand, and the number of leaf centers in each of the cells is tallied. From this information, $u_L(\vec{r})$ is computed for use in transport calculations. The spatial distribution of leaf area index $L(x,y)$ evaluated from $u_L(\vec{r})$ as

$$\int_0^{z_s} dz \; u_L(x,y,z) = L(x,y)$$

is shown in Figure 2. The heterogeneity of the distribution is evident with gaps between the trees. It may also be noted that in the space encompassing a tree the distribution of leaf area is highly variable. Thus, this requires a three-dimensional treatment of the radiation problem.

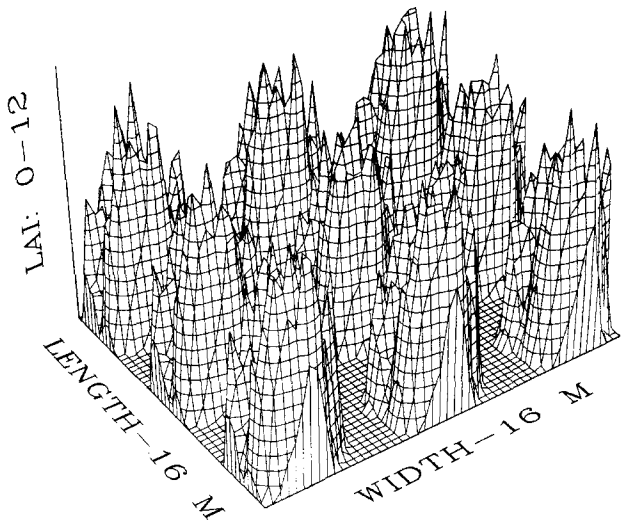

Figure 2. Spatial distribution of leaf area index in the hypothetical tree stand (Fig. 1). The parameters of the stand are discussed in the text. The leaf area index of the trees varied between 9.7 and 11.9; LAI of the entire stand is 6.9.

Leaf Normal Orientation Distribution

The orientation of leaves in a canopy can influence the radiation field, and, hence, it is essential to select a representative but simple model for the probability density of leaf normal orientation. It is often reasonable to assume that polar and azimuthal angles of the leaf normals are independent (Ross, 1981), that is, $g_L(\vec{r},\Omega_L)/2\pi = g_L(\vec{r},\mu_L)\, h_L(\vec{r},\phi_L)/2\pi$. For the inclination distribution $g_L(\vec{r},\mu_L)$ we use position-dependent models such as planophile, erectophile, plagiophile, and extremophile (de Wit, 1965). In case of a canopy characterized by a single leaf angle, $g_L(\vec{r},\mu_L) = \delta[\mu_L - \mu_L^*(\vec{r})]$. The leaf inclination distribution of many canopies can be described by the two-dimensional beta distribution (Strebel et al., 1985). The parameters of this distribution can be estimated empirically from measured leaf angle distributions; this scheme was also implemented in our 3D method.

Leaf Scattering Phase Function

A photon can either be specularly reflected at the surface of a leaf or can undergo reflection and refraction inside the leaf. Specular reflection from the leaves originates at the interface between air and the cuticular wax layer (Vanderbilt and Grant, 1985), and its magnitude can be computed from the incidence angle, the index of refraction, and characteristics of the surface wax layer. The leaf phase function for specular reflection is modeled by Fresenel equations averaged over polarization states, but corrected for optical roughness of the leaf (Myneni et al., 1990). On the other hand, once a photon reaches the inside of a leaf, it will undergo multiple reflections and refractions at the numerous cell wall–air interfaces, and can emerge in any direction with a probability given by Lambert's cosine law (Breece and Holmes, 1971; Brakke et al., 1989). This behavior can be modeled as a bi-Lambertian function (Shultis and Myneni, 1988), where a fraction r_D of the intercepted energy is reradiated in a cosine distribution about the leaf normal. Similarly, a fraction t_D is transmitted in a cosine distribution on the opposite side of the leaf. The leaf reflectance (r_D) and transmittance (t_D) are measured with integrating spheres and depend on the wavelength of the incident beam. These parameters are assumed given from measurements.

Results of Simulation

For the results reported in this section, a spatial grid of $50 \times 50 \times 10$ was used. Further, photons were allowed to stream in 48 directions; that is, an EQ_6 set was used. These values were based on our previous experience with the 3D method (Myneni et al., 1990). The four important results from the simulation are: 1) spatial distribution of spectral albedo $A(x,y)$, 2) spatial and angular distribution of canopy reflectance factor $R(x,y;\theta,\phi)$, 3) spatial distribution of upward and downward radiative fluxes $F_u(x,y,z)$ and $F_d(x,y,z)$, and 4) spatial distribution of the absorbed radiative flux $F_a(x,y,z)$.

The spatial distribution of spectral albedo (dimensionless) at near-infrared for the hypothetical plant stand discussed earlier is shown in Figure 3. The albedo was evaluated from the emerging intensities I^e as

$$A(x,y) = \frac{1}{F_{\text{in}}(x,y,0)} \int_0^{2\pi} d\phi \int_0^1 d\mu \;\; \mu I^e(\mu,\phi;x,y,0),$$

where F_{in} is the incident radiative flux

$$F_{\text{in}}(x,y,0) = \int_0^{2\pi} d\phi' \int_{-1}^{0} d\mu' |\mu'| [I_d(\Omega') + I_o \delta(\Omega' - \Omega_o)].$$

It is seen that the albedo distribution is strongly

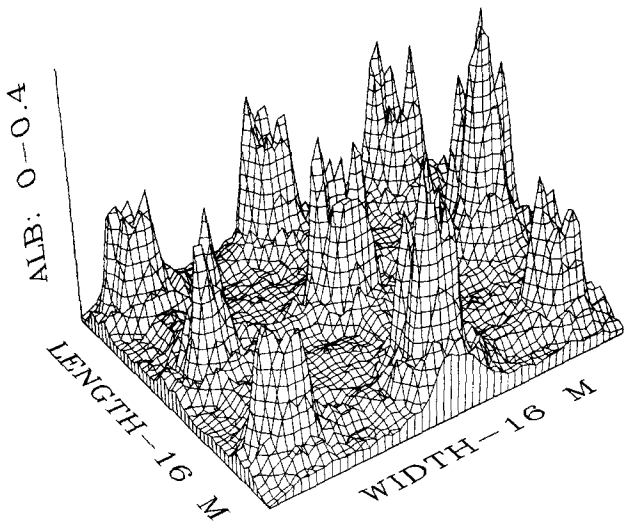

Figure 3. Spatial distribution of albedo in the near-infrared region of the hypothetical tree stand (Fig. 1). The incident radiation consisted of 80% monodirectional sunlight ($\theta_o = 150°$, $\phi_o = 45°$), and 20% isotropic diffuse skylight. The other parameters are discussed in the text.

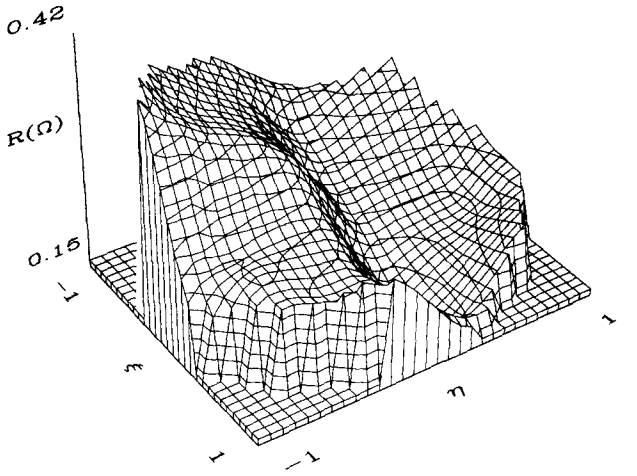

Figure 4. Spatially averaged angular distribution of reflectance factors in the near-infrared. Here $\xi \equiv (\sin\theta \cos\phi)$ and $\eta \equiv (\sin\theta \sin\phi)$ are the directional cosines of exiting direction Ω. The incident radiation consisted of 80% monodirectional sunlight ($\theta_o = 150°$, $\phi_o = 45°$), and 20% isotropic diffuse skylight. The other parameters are discussed in the text.

correlated with the spatial distribution of trees in the stand. A statistical analysis of this distribution should reveal the degree of autocorrelation, which, for instance, is important in the averaging of point measurements to obtain aggregate values (Jupp et al., 1988).

The reflectance factor (dimensionless), which is the ratio of the canopy radiance to that of an ideal reference panel (conservative Lambertian diffuser), both measured under identical illumination and viewing directions,

$$R(x,y;\theta,\phi) = \frac{\pi I^c(x,y,0;\theta,\phi)}{F_{in}(x,y,0)},$$

is shown in Figure 4 (averaged over the horizontal coordinates). The asymmetry of the distribution with enhanced backscatter and the bowl shape is characteristic of most plant stands; this has been experimentally verified as well (Deering, 1989).

The upward and downward radiative fluxes (W m^{-2}) are evaluated by summing the respective uncollided and collided radiation intensities. For instance, the downward flux is calculated as

$$F_d(\vec{r}) = \int_{2\pi^-} d\Omega\ |\mu| I_o \exp\left[\frac{1}{\mu}\tau_1(\vec{r},\Omega)\right]\delta(\Omega - \Omega_o) + \int_{2\pi^-} d\Omega\ |\mu| I_d(\Omega) \exp\left[\frac{1}{\mu}\tau_1(\vec{r},\Omega)\right] + \int_{2\pi^-} d\Omega\ |\mu| I^c(\vec{r},\Omega), \quad (8)$$

where $\mu < 0$. The first two terms in Eq. (8) denote uncollided direct sunlight and diffuse skylight. The last term denotes the scattered radiative flux. The difference between the upward and downward fluxes in a volume element is the net radiative energy available for plant functioning. Thus, these fluxes are the "linkage points" to an energy budget model.

In the evaluation of canopy photosynthesis, leaf-projected absorbed radiative flux F_a (W m^{-3}) in a volume element is required, apart from similar quantitites of uncollided incident fluxes. The quantity F_a is evaluated as

$$F_a(\vec{r}) = \int_{4\pi} d\Omega\ \sigma(\vec{r},\Omega)[1 - \omega(\vec{r},\Omega)] I^c(\vec{r},\Omega).$$

The feasibility of correlating the absorbed energy distribution (or the consequent photosynthetic rate) with reflectance factors (the remotely sensed observation) is to be discussed in a forthcoming paper (Myneni et al., 1991a).

INCLUSION OF THE HOT SPOT EFFECT

All rough and structured surfaces when illuminated by a directional radiative source with a wavelength considerably smaller than the size of the constituents of the surface show a local maximum of reflected radiation within a cone around the direction of retroillumination. When

observed precisely in the direction of incident radiation, only the illuminated parts of the canopy are seen, and hence the peak in the reflected intensity, called the hot spot (Kuusk, 1985; Asrar et al., 1989; Verstraete et al., 1990).

In radiative transfer one assumes that the scattering centers are far enough apart spatially such that each scattering center is in the far field of the radiation scattered from any other scattering center. However, this assumption is not satisfied in many vegetation canopies. Hence, cross-shadowing between leaves in a canopy leads to correlation in photon fates. This correlation is stronger between directions separated by a smaller angular spread than otherwise. The degree of correlation is dependent on the size distribution of the leaves and on the distribution of distances between the leaves. The correlated probability of photon attenuation and transport requires an alternate formulation (Myneni et al., 1991b). This theory leads to an equation set that is difficult to parameterize and compute. For the purposes of remote sensing, we developed a simple model for the hot spot effect and its inclusion in the 3D radiative transfer method is described here.

Consider the one-dimensional radiative transfer equation

$$-\mu\frac{\partial}{\partial z}I(z,\Omega)+\sigma(z,\Omega)I(z,\Omega)$$
$$=\int_{4\pi}d\Omega'\ \sigma_s(z,\Omega'\rightarrow\Omega)I(z,\Omega')+J(z,\Omega),$$

subject to the following boundary conditions:

$$I(0,\Omega)=0,\quad \mu<0,$$
$$I(Z_s,\Omega)=0,\quad \mu>0.$$

We consider the case of monodirectional solar illumination of the canopy, of intensity I_o incident in Ω_o ($\mu_o<0$). Also, we limit our interest to first-order collided intensities, for this constitutes a significant amount of energy that is contained in the hot spot (Kuusk, 1985). Thus, the equation of transfer is

$$-\mu\frac{\partial}{\partial z}I(z,\Omega)+\sigma(z,\Omega)I(z,\Omega)=\sigma_s(z,\Omega_o\rightarrow\Omega)I_o$$
$$\times\exp\left[-\frac{1}{|\mu_o|}\int_0^z dz'\ \sigma(z',\Omega_o)\right].$$

The solution of the above subject to stated boundary conditions is, for first-order collided intensity emerging at the top of the canopy in Ω ($\mu>0$),

$$I(0,\Omega)=\frac{I_o}{\mu}\int_0^{z_s}dz\ \sigma_s(z,\Omega_o\rightarrow\Omega)Q(z,\Omega_o,\Omega)\qquad(9)$$

where $Q(z,\Omega_o,\Omega)$ is the joint probability of viewing an element at depth z along the directions Ω_o and Ω, and is given by

$$Q(z,\Omega_o,\Omega)=\exp\left[-\frac{1}{|\mu_o|}\int_0^z dz'\ \sigma(z',\Omega_o)\right]$$
$$\times\exp\left[-\frac{1}{|\mu|}\int_0^z dz'\ \sigma(z',\Omega)\right]$$
$$=\exp[-\tau(z,\Omega_o)]\ \exp[-\tau(z,\Omega)].\qquad(10)$$

However, when $\Omega=-\Omega_o$, the probability of viewing the sunlit elements is unity, that is, $Q(z,\Omega_o,-\Omega)=\exp[-\tau(z,\Omega_o)]$, where $-\Omega_o$ is the retrosolar direction $(-\mu_o,\phi_o+\pi)$. But clearly Eq. (10) does not reduce to this form, because in radiative transfer all interaction events are assumed to be uncorrelated. Hence, the probability of a photon arriving at depth z along Ω_o and, the probability of a photon (when released in $-\Omega_o$ after interaction) traveling from depth z to outside are treated independently.

Kuusk (1985) using rigorous arguments derived an expression for the joint probability $Q(z,\Omega_o,\Omega)$ as

$$Q(z,\Omega_o,\Omega)=\exp\{-[\tau(z,\Omega)+\tau(z,\Omega_o)-\tau_p(z,\Omega_o,\Omega)]\},$$

where

$$\tau_p(z,\Omega_o,\Omega)=\sqrt{1/|\mu\mu_o|}$$
$$\times\int_0^z dz'\sqrt{\sigma(z',\Omega_o)\sigma(z',\Omega)}\gamma(z,\Omega_o,\Omega).$$

Here $\gamma(z,\Omega_o,\Omega)$ is the cross correlation function. Clearly, when $\Omega=-\Omega_o$, $\gamma\equiv1$, and $Q(z,\Omega_o,-\Omega=\exp[-\tau(z,\Omega_o)]$. Kuusk also presented several simple heuristic expressions for the function γ. However, it is not easy to formulate methods for determining γ for vegetation canopies.

To avoid using the cross correlation function directly, we begin by defining a bidirectional indicator function,

$$\Upsilon(\vec{r},\Omega',\Omega)=\begin{cases}1, & \text{if } \vec{r} \text{ can be viewed along } \Omega \text{ and } \Omega',\\ 0, & \text{otherwise.}\end{cases}$$

The joint probability of view can be evaluated by averaging over the realizations of the indicator function,

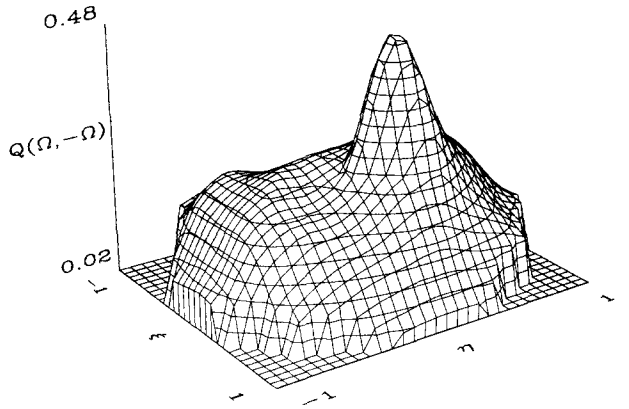

Figure 5. The joint probability Q of viewing an element at $z = 4.5$ m in the fractal tree stand ($Z_s = 10$ m). Here $\xi \equiv (\sin\theta \cos\phi)$ and $\eta \equiv (\sin\theta \sin\phi)$ are the directional cosines of exiting direction Ω. The solar zenith and azimuth angles are $180 - 21.24°$ and 225°; thus, the peak in the retrosolar direction—at zenith and azimuth angles of 21.24° and 45°.

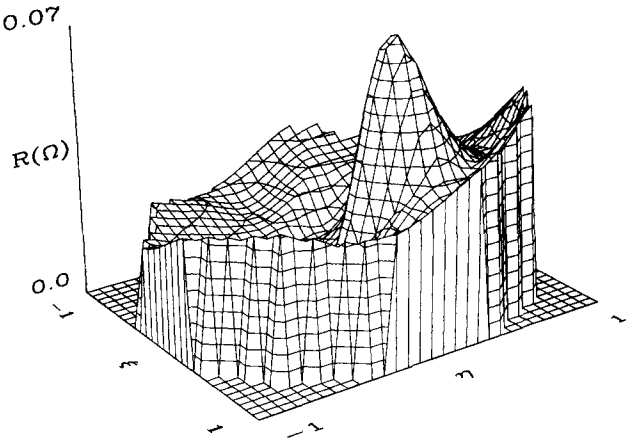

Figure 6. The angular distribution of reflectance factors in the red region of the spectrum simulated for the fractal tree stand (Fig. 1). Here $\xi \equiv (\sin\theta \cos\phi)$ and $\eta \equiv (\sin\theta \sin\phi)$ are the directional cosines of exiting direction Ω. The canopy is illuminated by monodirectional sunlight ($\theta_o = 158.76°$, $\phi_o = 225°$).

$$Q(z,\Omega',\Omega) = \frac{1}{N}\sum_{i=1}^{N} \Upsilon(z,\Omega,\Omega';x,y). \qquad (11)$$

The indicator function for the fractal tree stand described in the previous section can be determined by ray tracing, since the coordinates of all leaf centers, their orientation, and shape are known. The goal of ray tracing is to find the point of nearest intersection of a ray with an element in the scene. A ray $\vec{r}(t)$ can be described in vector form as $\vec{r}(t) = \vec{a} + t\vec{b}$, where the vector $\vec{a}$ is the origin of the ray, $\vec{b}$ is a vector in the direction of the ray, and t is a scalar. An element in the scene, a leaf, for instance, is described mathematically by the function $F(\vec{r}) = 0$. Substituting the former in F and solving for the smallest positive t gives the point of nearest intersection of the ray with the element. The calculation of the indicator function is accomplished in two steps. First, given the arguments of the indicator function, we determine two cylindrical volumes in the canopy which contain the leaf centers that can potentially intersect with the two rays. Second, the equations of these leaves in the reference frame are derived to estimate a realization of Υ.

The joint probability Q of viewing an element at $z = 4.5$ m in the fractal tree stand ($Z_s = 10$ m) is shown in Figure 5. The solar zenith and azimuth angles are $(180 - 21.24)°$ and 225°; thus, the peak in the retrosolar direction is at zenith and azimuth angles of 21.24° and 45°. It is now straightforward to evaluate the first-order radiation intensities exiting the stand [cf. Eqs. (9) and (11)] that include the hot spot effect [$I_H(\Omega)$]. In the spatially averaged discrete ordinates solution of the three-dimensional transport equation, the first-order collided intensity distribution is substituted with $I_H(\Omega)$. The presence of sky illumination and other boundary conditions necessitate appropriate modifications, but the principles are the same. The resulting angular distribution of the reflectance factors for the tree stand is shown in Figure 6. This pattern of strong backscattering with the hot spot around the retrosolar direction and weak forward scattering is unique to leaf canopies, and cannot be correctly simulated without a complete description of all the interactions.

VALIDATION WITH MEASUREMENTS

In this section results of comparision between the 3D method and experimental data collected independently over three different vegetation canopies are presented. Kimes et al. (1986) reported the directional reflectance distribution of a hardwood forest canopy measured as a function of solar position, from a helicopter platform using a hand-held radiometer with advanced very high resolution radiometer (AVHRR) Band 1 (0.58–0.68 μm) and Band 2 (0.73–1.1 μm). The hardwood canopy was spatially heterogeneous with a ground cover of 0.79. A 100 m × 100 m × 22 m

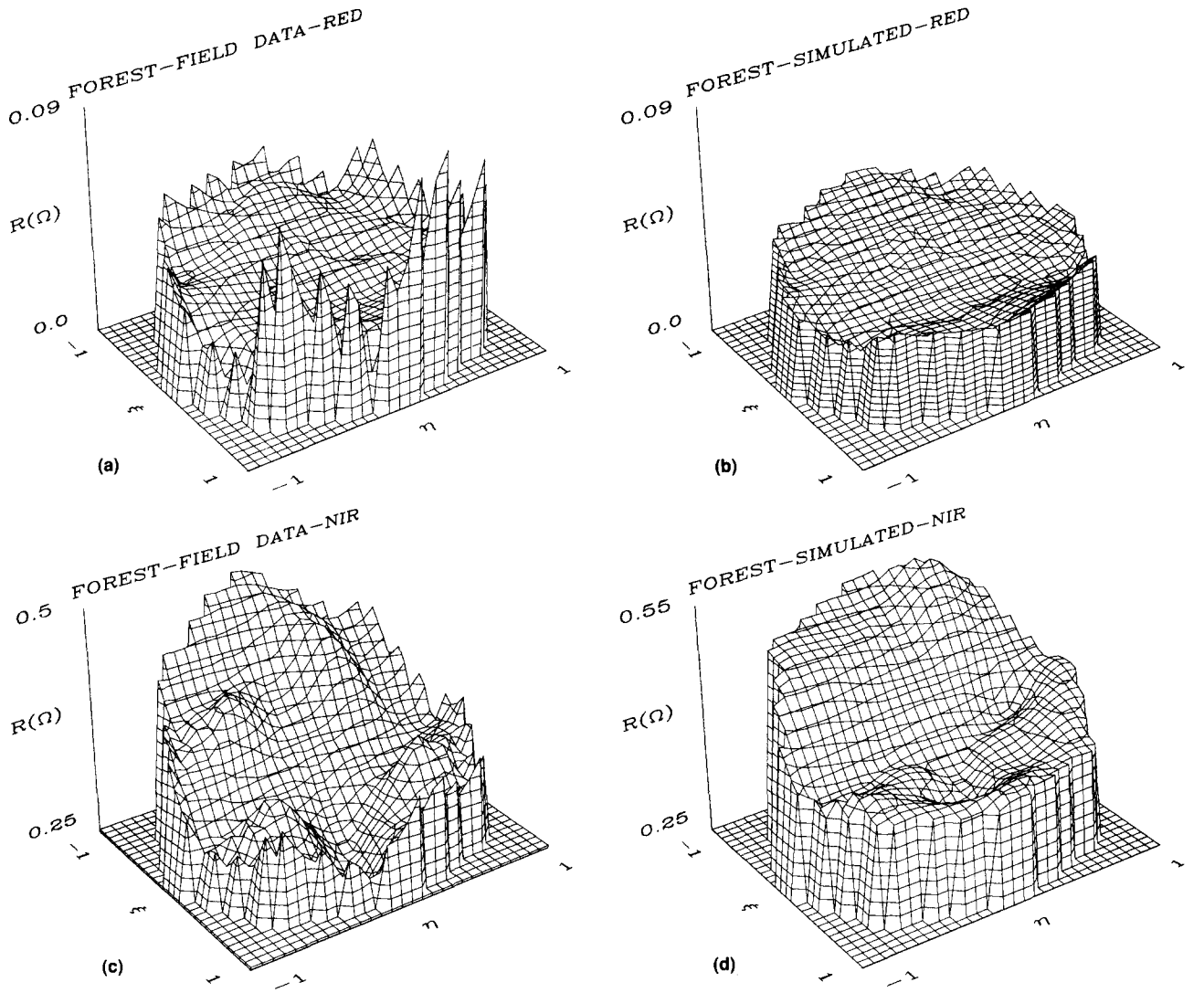

Figure 7. Hardwood forest canopy reflectance factors in the red (a,b) and near-infrared (c,d) regions. The measured data are of Kimes et al. (1986). Here $\xi \equiv (\sin\theta \cos\phi)$ and $\eta \equiv (\sin\theta \sin\phi)$ are the directional cosines of exiting direction Ω.

segment of this canopy with 316 randomly distributed trees was simulated. The mean dimensions of the trees was estimated to be 5 m × 5 m × 22 m. The reported standard deviation of the basal area of trees was used to statistically populate the stand about these mean dimensions. The leaf area index of the stand (4.2), the leaf normal orientation distribution, and the leaf and soil optical properties were also reported by Kimes et al. (1986). The mean leaf area index of the trees (5.32) was used to parameterize the quadratic model for leaf area density distribution function (Myneni et al., 1990). The proportion of direct sunlight in the total incident flux was assumed to be 0.8. A spatial grid of 50 × 50 × 10 and an angular grid of 48 directions was used in the discrete ordinates solution of the 3D radiative transfer equation. Other details regarding the site, experimental plan, and observations can be found in Kimes et al. (1986).

The observed and the simulated reflectance factors in Bands 1 and 2 are shown in Figures 7a–d. The zenith and azimuth of the sun were 135° and 0°, respectively. In all cases, the observed reflectance factors were limited to a maximum of 75° in view zenith angle (for practical considerations). We extrapolated these measurements to the full range (up to 90°), and, due to rather steep increase in Band 1 reflectance at oblique view angles, the spikes at highly oblique view zenith angles are artifacts of extrapolation (Fig. 7a). The simulated reflectance distributions

capture the overall trends in the measured data, however, in the strongly scattering near-infrared band, the maximum discrepency in the simulated results is an overestimate of ca. 10% (Figs. 7c,d).

The observed and simulated near-infrared to red reflectance ratios at solar zenith angles of 155° and 117° are shown in Figures 8 and 9 (plotted relative to solar azimuth). The symmetry about the solar principal plane can be seen in both observed and simulated distributions. At both sun positions, the simulated values are greater than measured values because of the overestimation of near-infrared reflectance; however, the degree of overestimation is less than 10%. In all cases, it can be seen that the simulated distributions are smoother than the measured distributions—a consequence of the idealization of canopy architecture in the simulation.

Ranson, et al. (1984) compiled a data set of soybean canopy architecture, optical properties, and directional reflectance factors with the intent of aiding validation of vegetation canopy reflectance models. The particular data set used here was collected on or around 17 July 1980, when ground cover was 0.72 and the canopy leaf area index was 3. A 50 m × 50 m × 0.7 m segment of the canopy with regularly spaced plants of size 0.55 m × 0.55 m × 0.7 m was simulated. The leaf normal orientation distribution and the leaf and soil optical properties were also reported by Ranson et al. (1984). The mean leaf area index of the plants (4.17) was used to parameterize the quadratic model for leaf area density distribution function (Myneni et al., 1990). A spatial grid of 50 × 50 × 10 and an angular grid of 48 directions was used in the discrete ordinates solution of the 3D radiative transfer equation. Other details regarding the field experiment can be found in Ranson et al. (1984). The observed and measured near-infrared (MSS Band 4) to red (MSS Band 2) reflectance ratios at a sun zenith angle of 160° and azimuth of 15° are shown in Figures 10a and 10b. Although the simulated results are overestimates (ca. 10%), the 3D method captures the overall trends and shape of the observed surface.

A final validation of the 3D method was made with a data set of maize canopy architecture, optical properties, and directional reflectance factor distributions reported by Ranson and Biehl (1983). The maize plants were planted in rows

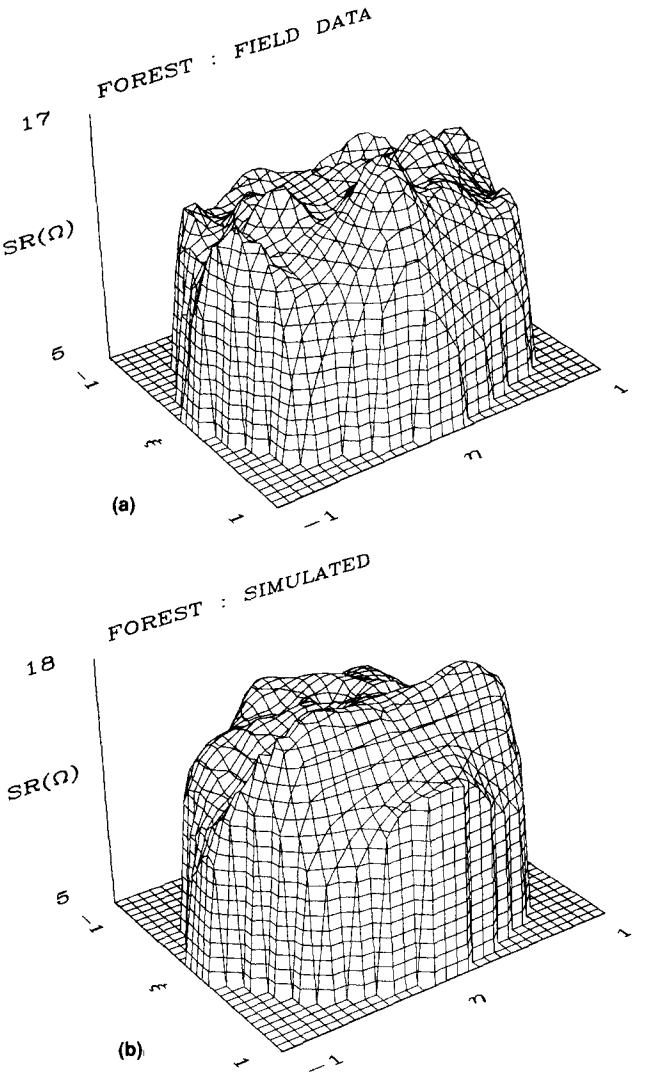

Figure 8. Ratio of hardwood forest canopy reflectance factor in the near-infrared to red (SR) for a sun zenith angle of 155°. The measured data (a) are of Kimes et al. (1986). Here $\xi \equiv (\sin\theta \cos\phi)$ and $\eta \equiv (\sin\theta \sin\phi)$ are the directional cosines of exiting direction Ω.

of width 0.72 m, and between-plant spacing of 0.22 m. An 80 m × 80 m × 2.7 m segment of the canopy was simulated with plants of dimensions 0.6 m × 0.4 m × 2.7 m, and leaf area index of 4. The leaf normal orientation distribution and the leaf and soil optical properties were also reported by Ranson and Biehl (1983). The quadratic model for plant leaf area density was used. A spatial grid of 50 × 50 × 10 and an angular grid of 48 directions was used in the discrete ordinates solution of the 3D radiative transfer equation. The observed and simulated near-infrared (TM Band

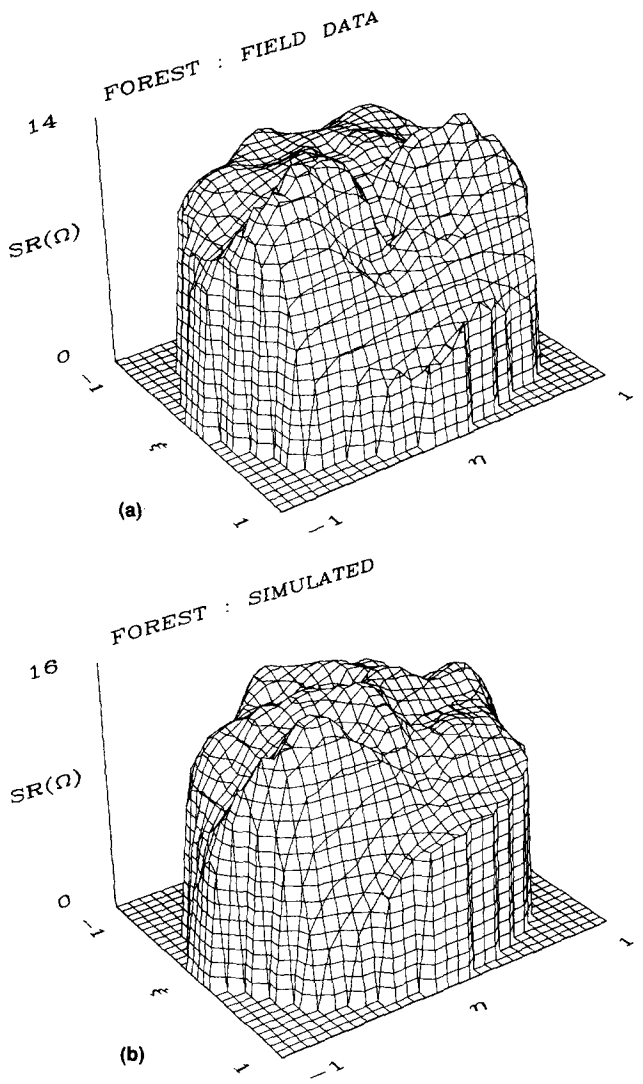

Figure 9. Ratio of hardwood forest canopy reflectance factor in the near-infrared to red (SR) for a sun zenith angle of 117°. The measured data (a) are of Kimes et al. (1986). Here $\xi \equiv (\sin\theta \cos\phi)$ and $\eta \equiv (\sin\theta \sin\phi)$ are the directional cosines of exiting direction Ω.

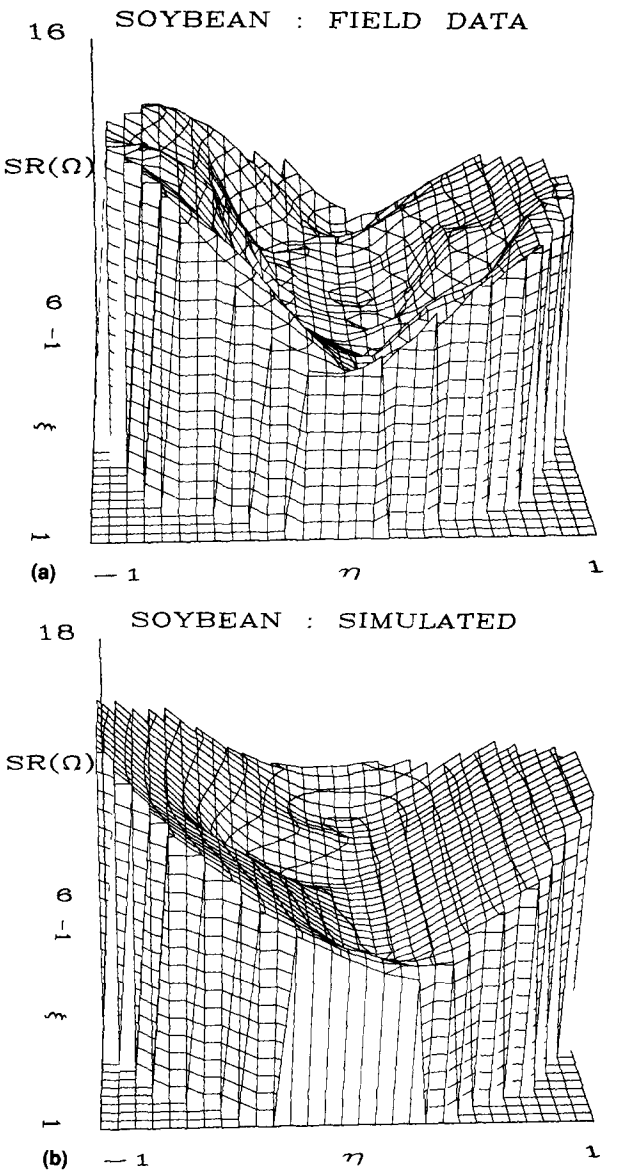

Figure 10. Ratio of soybean canopy reflectance factor in the near-infrared to red (SR) for a sun zenith angle of 160°. The measured data (a) are of Ranson et al. (1984). Here $\xi \equiv (\sin\theta \cos\phi)$ and $\eta \equiv (\sin\theta \sin\phi)$ are the directional cosines of exiting direction Ω.

4) to red (TM Band 3) reflectance ratios are shown in Figures 11a and 11b. The sun zenith (azimuth) angle ranged between 140° and 145° (285° and 291°) during data aquisition; mean values were used in the simulation. As in the previous cases, the simulated surface is smoother, with a maximum discrepency of ca. 10%.

From the above-presented comparisions, the following conclusions can be drawn. The 3D method based on radiative transfer thoery satisfactorily simulates the directional reflectance distributions of spatially heterogeneous vegetation canopies. In particular, the anisotropy of the distribution with its characteristic enhanced backscatter and decreased forward scatter, are well captured by the method. However, the method generally overestimates near-infrared reflectance, for some directions by about 10%. Also, the simulated angular distributions are smooth, while the measured distributions exhibit the natural variability, that is, ridges, local valleys, troughs, etc.; the reasons for this are not clear. It could be

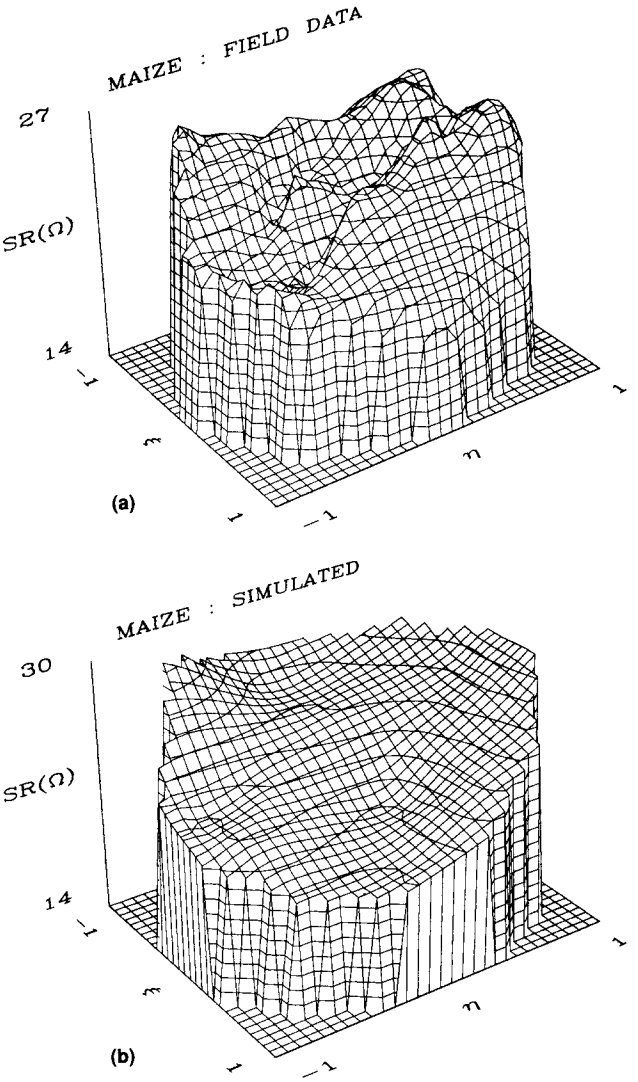

Figure 11. Ratio of maize canopy reflectance factor in the near-infrared to red (SR) for a sun zenith angle of 142.5°. The measured data (a) are of Ranson and Biehl (1983). Here $\xi \equiv (\sin\theta \cos\phi)$ and $\eta \equiv (\sin\theta \sin\phi)$ are the directional cosines of exiting direction Ω.

due to variability inherent in the target. Also, all natural vegetation communities exhibit clumping of foliage elements, which decreases radiation capture and consequently the canopy reflectivity. The fractal tree model presented here can, in principle, account for clumping of foliage, but at the present time we do not have data with which to parameterize it.

The work reported here was made possible through NASA Grant NAS5-30442; we gratefully acknowledge this support. We thank Dr. Kimes, Dr. Ranson, and their co-workers for providing the data sets used in the validation of the 3D method.

REFERENCES

Alcouffe, R. E. (1990), A diffusion-accelerated S_n transport method for radiation transport on a general quadrilateral mesh, *Nucl. Sci. Eng.* 105:191–197.

Asrar, G., Myneni, R. B., and Kanemasu, E. T. (1989), Estimation of plant-canopy attributes from spectral reflectance measurements, in *Theory and Applications of Optical Remote Sensing* (G. Asrar, Eds.), Wiley, New York, pp. 252–296.

Brakke, T. W., Smith, J. A., and Harnden, J. M. (1989), Bidirectional scattering of light from tree leaves, *Remote Sens. Environ.* 29:175–183.

Breece, H. T., and Holmes, R. A. (1971), Bidirectional scattering characteristics of healthy green soybean and corn leaves *in vivo*, *Appl. Opt.* 10:119–127.

Bunnik, N. J. J. (1978), The multispectral reflectance of shortwave radiation by agricultural crops in relation with their morphological and optical properties, Pudoc Publ., Wageningen, The Netherlands.

Carlson, B. G., and Lathrop, K. D. (1968), Transport theory: the method of discrete ordinates, in *Computing Methods in Reactor Physics* (H. Greenspan, C. N. Kelber, and D. Okrent, Eds.), Gordon and Breech, New York, pp. 167–265.

Choudhury, B. J. (1987), Relationships between vegetation indices, radiation absorption, and net photosynthesis evaluated by a sensitivity analysis, *Remote Sens. Environ.* 22: 209–233.

Deering, D. W. (1989), Field Measurements of Bidirectional Reflectance, in *Theory and Applications of Optical Remote Sensing* (G. Asrar, Eds.), Wiley, New York, pp. 14–61.

de Wit, C. T. (1965), *Photosynthesis of Leaf Canopies*, Pudoc Publ., Wageningen, The Netherlands.

Dickinson, R. E. (1983), Land surface processes and climate-surface albedos and energy balance, *Adv. Geophys.* 25: 305–353.

Ganapol, B. D., and Myneni, R. B. (1991), The F_N method for the one-angle radiative transfer equation applied to plant canopies, *Remote Sens. Environ.*, 39:213–231.

Gerstl, S. A. W., and Zardecki, A. (1985), Coupled atmosphere / canopy model for remote sensing of plant reflectance features, *Appl. Opt.* 24:94–103.

Goel, N. S. (1988), Models of vegetation canopy reflectance and their use in estimation of biophysical parameters from reflectance data, *Remote Sens. Rev.* 4:1–222.

Gutschick, V. P., and Wiegel, F. W. (1984), Radiation transfer in vegetation canopies and layered media: Rapidly solvable exact integral equation not requiring Fourier resolution, *J. Quant. Spectrosc. Radiat. Transfer* 31:71–82.

Hall, F. G., Huemmrich, K. F., and Goward, S. N. (1990), Use of narrow-band spectra to estimate the fraction of absorbed photosynthetically active radiation, *Remote Sens. Environ.* 28:47–54.

Jupp, D. L. B., Strahler, A. H., and Woodcock, C. E. (1988), Autocorrelation and regularization in digital images. I. Basic theory, *IEEE Trans. Geosci. Remote Sens.* GE-26: 463–473.

Kimes, D. S., and Kirchner, J. A. (1982), Radiative transfer model for heterogeneous 3D scenes, *Appl. Opt.* 21:4119–4129.

Kimes, D. S., Newcomb, W. W., Nelson, R. F., and Schutt, J. B. (1986), Directional reflectance distributions of a hardwood and pine forest canopy, *IEEE Trans. Geosci. Remote Sens.* GE-24:281–293.

Kuusk, A. (1985), The hot spot effect of a uniform vegetative cover, *Sov. J. Remote Sens.* 3:645–658.

Lathrop, K. D. (1976), THREETRAN: a program to solve the multigroup discrete ordinates transport equation in (x,y,z) geometry, USAEC Rep. LA-6333-MS, Los Alamos National Laboratory, Los Alamos, NM.

Lewis, E. E., and Miller, W. F., Jr. (1984), *Computational Methods of Neutron Transport*, Wiley-Interscience, New York.

Li, X., and Strahler, A. H. (1986), Geometrical-Optical bidirectional modelling of a coniferous forest canopy, *IEEE Trans. Geosci. Remote Sens.* GE-24:906–919.

Marshak, A. L. (1989), Consideration of the effect of hot spot for the transport equation in plant canopies, *J. Quant. Spectrosc. Radiat. Transfer* 42:615–630.

Myneni, R. B. (1991), Modeling radiative transfer and photosynthesis in three dimensional vegetation canopies, *Agric. For. Meteorol.* 55:323–344.

Myneni, R. B., Ross, J., and Asrar, G. (1989), A review on the theory of photon transport in leaf canopies in slab geometry, *Agric. For. Meteorol.* 45:1–153.

Myneni, R. B., Asrar, G., and Gerstl, S. A. W. (1990), Radiative transfer in three dimensional leaf canopies, *Trans. Theory Stat. Phys.* 19:205–250.

Myneni, R. B., Ganapol, B. D., and Asrar, G. (1991a), Remote sensing of vegetation canopy photosynthetic and stomatal conductance efficiencies, *Remote Sens. Environ.*, forthcoming.

Myneni, R. B., Marshak, A. L., and Knyazikhin, Yu. V. (1991b), Transport theory for a leaf canopy of finite dimensional scattering centers, *J. Quant. Spectrosc. Radiat. Transfer*, 46:259–280.

Pomraning, G. C. (1973), *The Equations of Radiation Hydrodynamics*, Pergamon, Oxford.

Ranson, K. J., and Biehl, L. L. (1983), Corn canopy reflectance modelling data set, LARS Tech. Rep., Purdue Univ., W. Lafayette, IN.

Ranson, K. J., Biehl, L. L., and Daughtry, C. S. T. (1984), Soybean canopy reflectance modelling data set. LARS Tech. Rep. 071584, Purdue Univ., W. Lafayette, IN.

Ross, J. (1981), *The Radiation Regime and Architecture of Plant Stands*, Dr. W. Junk Publ., The Hague, The Netherlands.

Ross, J., and Marshak, A. L. (1988), Calculation of canopy bidirectional reflectance using the Monte Carlo method, *Remote Sens. Environ.* 24:213–225.

Sellers, P. (1985), Canopy reflectance, photosynthesis and transpiration, *Int. J. Remote Sens.* 8:1335–1372.

Shultis, J. K., and Myneni, R. B. (1988), Radiative transfer in vegetation canopies with anisotropic scattering, *J. Quant. Spectrosc. Radiat. Transfer* 39:115–129.

Simmer, C., and Gerstl, S. A. W. (1985), Remote sensing of the angular characteristics of canopy reflectance, *IEEE Trans. Geosci. Remote Sens.* GE-23:648–655.

Strebel, D. E., Goel, N. S., and Ranson, K. J. (1985), Two-dimensional leaf orientation distributions, *IEEE Trans. Geosci. Remote Sens.* GE-23:640–647.

Suits, G. W. (1972), The calculation of the directional reflectance of a vegetative canopy, *Remote Sens. Environ.* 2: 117–125.

Vanderbilt, V. C., and Grant, L. (1985), Plant canopy specular reflectance model, *IEEE Trans. Geosci. Remote Sens.* GE-23:722–730.

Verhoef, W. (1984), Light scattering by leaf layers with application to canopy reflectance, *Remote Sens. Environ.* 16:125–141.

Verstraete, M. M., Pinty, B., and Dickinson, R. E. (1990), A physical model of the bidirectional reflectance of vegetation canopies. 1. Theory, *J. Geophys. Res.* 95:11755–11765.

Welles, J. M., and Norman, J. M. (1991), Photon transport in discontinuous canopies: A weighted random approach, in *Photon-Vegetation Interactions: Applications in Optical Remote Sensing and Plant Ecology* (R. B. Myneni and J. Ross, Eds.), Springer-Verlag, Heidelberg, pp. 389–414.